ELSEVIER

Journal of Chromatography A, 910 (2001) 31–49

JOURNAL OF CHROMATOGRAPHY A

www.elsevier.com/locate/chroma

Computer-assisted high-performance liquid chromatography method development with applications to the isolation and analysis of phytoplankton pigments

Laurie Van Heukelem*, Crystal S. Thomas

University of Maryland Center for Environmental Science, Horn Point Laboratory, P.O. Box 775, Cambridge, MD 21613, USA

Received 29 August 2000; received in revised form 7 November 2000; accepted 10 November 2000

Abstract

We used chromatography modeling software to assist in HPLC method development, with the goal of enhancing separations through the exclusive use of gradient time and column temperature. We surveyed nine stationary phases for their utility in pigment purification and natural sample analysis. For purification, a complex algal matrix was separated on an efficient monomeric column, from which partially purified fractions were collected and purified on polymeric columns that exaggerated resolution between pigments of interest. Additionally, we feature an HPLC method that is simple, fast, demonstrates excellent transferability and is ideal for quantitative analysis of pigments in dilute natural water samples.

Keywords: Chromatography modeling software; Stationary phases, LC; Phytoplankton pigments; Carotenoids; Chlorophylls

1. Introduction

HPLC methods for the analysis of phytoplankton pigments are used to help assign algal species to phylogenetic divisions, assess phytoplankton abundance and diversity in natural samples [1] and provide information on photosynthetic and photoprotective physiology [2]. However, no one method can resolve all pigments important to these purposes as there are many pigments to separate and as pigment separations are improved, new pigments are often identified. Several approaches have been used to improve pigment separations as recently reviewed by Jeffrey et al. [1]. These approaches have included the use of ternary solvent systems (using three pumps) [3,4], C_{18} columns [3–16] and C_8 columns [17–20] and manipulations to column temperature (T) [9,13–16,20]. The C_{30} stationary phase has been useful in the analysis of pigments in food and tissues as recently reviewed [21] and has had limited use thus far in the analysis of phytoplankton pigments [22,23]. A very promising new method which utilizes a pyridine-containing mobile phase and a C_8 column separates many pigments not previously resolved and has been used to identify the elution position of many new pigments [20]. We used an alternative approach to improve separations: the combined use of column T and gradient time (t_G), in conjunction with a simple binary solvent system. Our approach was enabled by method development software.

*Corresponding author. Fax: +1-410-221-8490.
E-mail address: laurievh@hpl.umces.edu (L. Van Heukelem).

0378-4347/01/$ – see front matter
PII: S0378-4347(00)00603-4

The software selected (DryLab, from LC Resources, Walnut Creek, CA, USA) has been successfully used [24] to optimize separations of 14 different sample types, including the separation of 29 algal pigments. To use this software, retention times (t_R) are recorded for a suite of compounds analyzed on the same HPLC column under four chromatographic conditions, including two values each of t_G and T. From the observed t_R values (referred to as input data), the software predicts the t_R values which would result from hypothetical chromatographic conditions selected by the user (including such things as t_G, gradient shape, column T, column dimensions and flow-rate (F)). The conditions required for optimal separations can then be easily identified.

Our ultimate goals in using this software were to identify methods which would enhance our abilities to isolate pigments as standards from natural sources and to identify a method that would simultaneously separate as many important pigments as possible and be suitable for the routine quantitative analysis of pigments in natural water samples. Additional requirements of this latter method were that it be based on a simple methanol-based binary solvent system, use linear gradients only, have a short analysis time and excellent detectability and be easily transferred to other instruments. We collected pigment t_R data from nine different columns for use with the simulation software. We used changes to values of T and t_G for optimizing conditions as we wanted to see how effectively we could improve separations based exclusively on these two variables.

We identify columns and methods well suited to the isolation of pigments from algal monocultures for use as pigment standards and we introduce a new method where we describe the elution position of 57 algal pigments.

2. Experimental

2.1. Equipment and software

A Hewlett-Packard (HP, Waldbronn, Germany) series 1100 HPLC system with autoinjector (900 μl syringe head), refrigerated autosampler compartment, thermostatted column compartment, quaternary pump with in-line vacuum degasser, and photo-diode array detector set to monitor 450 and 665 nm (both with 20 nm bandwidths) was used for primary studies. In-line photo-diode array spectra (from 350 to 700 nm) was collected for each pigment (Table 1) and compared with published values [20,25] for pigment identifications. Dwell volume was 3 ml. A Beckman (Beckman Coulter, Fullerton, CA, USA) System Gold HPLC was equipped with a dual pump (125 solvent module), photo-diode array detector set to monitor 450 nm, manual injector (200 μl loop), and an external column heating device (Eldex Laboratories, Napa, CA, USA). Dwell volume was 2.2 ml.

Chromatography modeling software (DryLab, version 2.05, LC Resources, Walnut Creek, CA, USA) was donated for use. This software requires (for predictions based on simultaneous variation of column T and t_G) retention times gathered from four sets of conditions, referred to as the input data (Table 2, further details in Section 3.1). We used t_R values for pigments in various algal culture and mutant corn leaf extracts for input data. After developing suitable methods for pigment isolation, we isolated pigments for use as standards and then recombined them into one standard test mixture containing 33 pigments. This mixture was used in subsequent testing.

After the chromatography modeling software was used to generate hypothetical conditions for the best separation, those conditions were implemented on the HPLC. For these analyses, an injector program was used which mixed sample with buffer (28 m*M* tetrabutyl ammonium acetate (TBAA), pH 6.5) in the sample loop before injection. With the Beckman Gold HPLC and when using large injection volumes (900 μl) on the HP HPLC (during pigment isolations), sample was premixed by hand with buffer and then allowed to equilibrate for 5 min before injecting. All samples were equilibrated to the autosampler compartment temperature (5°C) of the HP HPLC before injecting.

2.2. Materials

2.2.1. Reagents and solvents

All reagents except ethanol (JT Baker, Phillipsburg, NJ, USA) were HPLC grade: methanol (EM Science, Gibbstown, NJ, USA or JT Baker), acetone

Table 1
Pigments, SCOR abbreviations used in the text, code (number or letter) used to identify elution position of pigments in Figs. 2–9 and the pigment sources used to document retention time (t_R) values are shown[a]

Code		Pigment name	SCOR [26] WG 78 abbreviation	Source[b]	t_R (min)	R_s (peak code)	Visible absorbance spectra (nm)
1	*	Chlorophyll *c*3	chl *c*3	C J L N S T	3.88		456, 588 (625)
2		Monovinyl chl *c*3	MV chl *c*3	J	4.14		448, 585 (626)
3	*	Chlorophyll *c*2	chl *c*2	A–E H J L–O R–T	5.70	NR 3/4	446, 584, 634
4	*	Mg 3,8-divinyl pheoporphyrin a_5 monomethyl ester	Mg DVP	G P	5.81	NR 4/a	440, 576, 632
a		Unknown	–	K	5.92	NR a/5	–
5	*	Chlorophyll *c*1	chl *c*1	B D E R	6.05	NR 5/6	442, 580, 634, 668
6		Chlorophyllide *a*	chlide *a*	F H N O	6.06		(390), 434, 620, 668
7	**	Peridinin	perid	A B M	9.32		476
8		Peridinin isomer	–	A B M	9.58		478
b		Unknown	–	P	11.37		456, 476
9	**	19′-Butanoyloxy fucoxanthin	but-fuco	VKI[c] C N S T	12.31		448, 464
c		Unknown	–	G	12.68	NR c/10	458
10	**	Fucoxanthin	fuco	C D E L N R S T	12.63		454
11	**	Neoxanthin	neo	F G P U	13.29	NR 11/12	414, 438, 466
12		4-Keto-19′-hexanoyloxyfucoxanthin	4 k-hex-fuco	J	13.31		448, 470
d		Unknown	–	L	13.73	NR d/13	446, 468
13	**	Prasinoxanthin	pras	VKI[c] G P	13.74		462
14	**	Violaxanthin	viola	VKI[c] F G P Q U	13.99	R_s = 1.3, 14/15	418, 442, 470
15	**	19′-Hexanoyloxy fucoxanthin	hex-fuco	VKI[c] C J L	14.16		(430), 452, 480
16	*	Astaxanthin	asta	shrimp carapace G	14.53		480
e		Unknown	–	P	14.78		466
17		Diadinochrome	diadchr	M	15.02	NR 17/f	(410), 428, 456
f		Unknown	–	J	15.09	NR f/18	448, 470
18		Unknown (myxo-like spectra)	–	K	15.13	NR 18/19	452, 474, 506
19	*	Diadinoxanthin	diadino	A–E J L–N R–T	15.23	R_s = 1.4, 19/20	(428), 446, 476
20		Dinoxanthin	dino	A M	15.49		416, 440, 470
21	*	Antheraxanthin	anth	F	15.99		(425), 446, 474
22	**	Alloxanthin	allo	H O	16.53		(430), 452, 480
23	*	Diatoxanthin	diato	C D E M R T	17.12	NR 23/24	(430), 454, 480
24		Monadoxanthin	monado	H O	17.22		(422), 444, 472
25	**	Zeaxanthin	zea	C F G I K P Q V	17.79		(430), 452, 478
26	**	Lutein	lut	F G T V	17.98		424, 446, 474
g		Unknown	–	Q	18.24	NR g/h	422, 444, 472
h		Unknown	–	G	18.32		(408), 428, 454
i		Unknown	–	L N S T	18.84		(424), 448, 472
27	**	Canthaxanthin	cantha	W	19.07		480
j		Unknown	–	Q	19.23		422, 444, 472
28	*	Gyroxanthin diester-like 1 [27]	–	C	19.94		(426), 444, 472
29	*	Gyroxanthin diester-like 2 [27]	–	C	21.00		(426), 444, 472
30	*	Divinyl chlorophyll *b*	DV chl *b*	U	21.92	R_s = 0.8, 30/31	478, 608, 654
31	**	Monovinyl chlorophyll *b*	chl *b*	Fluka[d] F G P	22.03		468, 602, 652
32		Divinyl chlorophyll *b*′	DV chl *b*′	U	22.29		480, 608, 658
33		Crocoxanthin	croco	H O	22.42	NR 33/34	(428), 446, 476
34		Monovinyl chlorophyll *b*′	chl *b*′	Fluka[d] F G P	22.50		470, 602, 652
35		Chlorophyll *a* allomer 1	chl *a* allom	Fluka[d] A–T	23.30		(390), 432, 620, 666
36		Chlorophyll *a* allomer 2	chl *a* allom	Fluka[d] A–T	23.43	NR 36/k	(390), 432, 620, 666
k		Unknown	–	R	23.52	NR k/L	(464–474)
L		Unknown	–	R	23.52	NR L/37	454

Table 1. Continued

Code		Pigment name	SCOR [26] WG 78 abbreviation	Source[b]	t_R (min)	R_s (peak code)	Visible absorbance spectra (nm)
37		Phytylated chlorophyll *c*-like	phytyl-chl *c*	J R	23.53		460, 588, 636
38	**	Divinyl chlorophyll *a*	DV chl *a*	U	23.76		(390), 442, 622, 666
m		Unknown	–	L	23.91	NR m/39	458, 588, 638
39	**	Monovinyl chlorophyll *a*	chl *a*	Fluka[d] A–T	23.96		(390), 432, 620, 666
40		Divinyl chlorophyll *a′*	DV chl *a′*	U	24.13		(386), 440, 622, 666
41		Monovinyl chlorophyll *a′*	chl *a′*	Fluka[d] A–T	24.33		(388), 432, 618, 666
n		Unknown	–	P	25.58		(422), 442, 470
42	*	β,ε-Carotene (α-carotene)[e]	β,ε-car	Sigma[f] G H J L O P S	26.65	NR 42/43	(422), 446, 474
43	*	β,β-Carotene (β-carotene)[d]	β,β-car	Fluka[d], A–G, I–N P–U	26.71		(430), 452, 476

[a] Pigments with * or ** were used with all columns (t_R and R_s data given are specific to the method described in Section 3.6). R_s is ≥1.5 unless otherwise noted (NR = R_s < 1.0). Visible absorbance spectra was obtained from the in-line HPLC photo-diode array detector (350–700 nm) (solvent A, 70:30 methanol, 28 m*M* TBAA, pH 6.5; solvent B, methanol). Parentheses indicate spectral shoulder.

[b] Sources: Horn Point batch cultures, (A) *Prorocentrum minimum*, (B) *Gyrodinium uncatenum*, (C) *Gyrodinium galatheanum*, (D) *Thalassiosira pseudonana*, (E) *Isochrysis* sp. (TISO strain, CCMP 1324), (F) *Dunaliella tertiolecta* (CCMP 1320), (G) *Pycnococcus provasolii* (CCMP 1203), (H) *Pyrenomonas salina*, (I) *Synecoccocus sp.*; CCMP individual cultures, (J) *Emiliania huxleyi* (CCMP 373), (K) *Synechococcus* cf. *elongatus* (CCMP 1629), (L) *Chrysochromulina polyepsis* (CCMP 1757), (M) *Amphidinium carterae* (CCMP 1314), (N) *Pelagococcus subviridis* (CCMP 1429), (O) *Guillardia theta* (CCMP 327), (P) *Micromonas pusilla* (CCMP 1545), (Q) *Nannochoropsis* sp. 1 (CCMP 531), (R) *Isochrysis galbana* (CCMP 1323); all other sources, (S) *Pelagamonas calceolata*, (T) *Aureococcus anophagefferens*, (U) mutant corn, (V) marigold petals, (W) gift from Perdue, Salisbury, MD, USA.

[c] VKI Water Quality Institute, Denmark.

[d] Fluka (Milwaukee, WI, USA).

[e] Trivial name.

[f] Sigma (St. Louis, MO, USA).

(EM Science), ammonium acetate (JT Baker) and 0.4 *M* tetrabutyl ammonium hydroxide titrant (JT Baker). Water was deionized and filtered. Solvent A was 70:30 (v/v) methanol, 28 m*M* aqueous TBAA, pH 6.5. Solvent B was methanol or ethanol (Table 2).

Table 2
Chromatographic conditions used for generating pigment t_R databases for use with DryLab chromatography modeling software[a]

Column	Column dimensions (mm)	Column temperatures (°C)	Gradient times (min)	Initial %B	Flow rate (ml/min)
C_8 columns					
Hypersil mos-2	100×4.6	40, 60	15, 45	5	1.0
Luna C_8 (2)	100×4.6	40, 60	15, 45	5	0.8
Eclipse XDB	150×4.6	45, 60	20, 60	0	1.0
C_{18} columns					
Supelcosil LC 318	250×4.6	45, 60	20, 60	5	1.0
Supelcosil LC PAH	100×4.6	45, 60	15, 45	5	1.0
Vydac 201TP	250×3.2	45, 60	20, 60	0	0.6
YMC ODS-AL	150×4.6	40, 60	20, 60	5	1.0
Zorbax Bonus-RP C_{14}	250×4.6	45, 60	20, 60	0	1.2
YMC C_{30}	250×4.6	40, 60	20, 60	20	1.0

[a] Pigments were analyzed on each column at two values of *T* and two values of t_G. All gradients were linear from the specified initial percent solvent B to 100% solvent B. Solvent A, 70:30 methanol, 28 m*M* TBAA, pH 6.5; solvent B, methanol, except for the YMC C_{30} column where it was ethanol. Flow-rates were adjusted to keep backpressure below 180 bar.

2.2.2. Columns

Ten different reversed-phase, silica-based columns were used in this study. Aliphatic chain length and physical characteristics varied (Table 3). The Supelcosil LC318 C_{18} was used in two dimensions: 250×4.6 mm for computer modeling work and 100×4.6 mm for pigment isolations.

2.2.3. Algal cultures

Algal cultures with well characterized pigment content were used for the isolation of pigment standards and for collecting input data. They were (their clonal designation is indicated when known): (1) *Dunaliella tertiolecta* (CCMP 1320), (2) *Pycnococcus provasolii* (CCMP 1203), (3) *Synechococcus* sp., (4) *Isochrysis* sp. (T.ISO strain, CCMP 1324), (5) *Gyrodinium uncatenum*, (6) *Prorocentrum minimum*, (7) *Thalassiosira pseudonana*, (8) *Pyrenomonas salina* and (9) *Gyrodinium galatheanum*. These cultures were grown in large batches at Horn Point Laboratory, harvested onto glass fiber filters and frozen at −75°C until used. Additional cultures used with the new method on the Eclipse XDB C_8 column were grown at Provasoli-Guillard National Center for Culture of Marine Phytoplankton (CCMP), harvested onto GF/F filters, frozen immediately in liquid nitrogen and shipped to Horn Point Laboratory.

2.2.4. Pigment standards

The Scientific Committee on Oceanic Research (SCOR) abbreviations will be used throughout when referring to pigments (Table 1). We purchased β,ϵ-car (discontinued, Sigma), β, β-car (Fluka), chl *a* (Fluka) and chl *b* (Fluka). Lut (isolated from marigold petals) and cantha were donated by Perdue. Other pigments were either isolated from algal monocultures, mutant maize leaves grown in our laboratory [28] or shrimp carapace.

Standard concentrations (after transfer to the solvent required for use with the appropriate extinction coefficients) were determined using a dual beam spectrophotometer (model U-3110, Hitachi, Tokyo, Japan), bandwidth 2 nm, corrected for absorbance at 750 nm [29]. Spectrophotometer accuracy was assessed using NIST traceable neutral density filters (Starna Cells, Atascadero, CA, USA). Standards were stored at −20°C in darkness in amber bottles with PTFE-lined lids or PTFE bottles.

2.2.5. Sample extraction

Algal monocultures and field samples were collected on glass fiber filters and extracted in acetone (90 or 100%) or ethanol (as with some cultures used for pigment isolations). Samples were chilled while disrupted with an ultrasonic probe (model 450, Branson Ultrasonics, Danbury, CT, USA). Extracts

Table 3
Physical characteristics of HPLC columns evaluated[a]

Column name	Dimensions (mm)	Particle size (μm)	Surface area (m^2/g)	Pore size (Å)	Endcapped	% Carbon load, bonding chemistry	pH tolerance
Eclipse® XDB C_8[b]	150×4.6	3.5	180	80	Yes	7.6, monomeric	2–9
Hypersil® C_8 mos-2[c]	100×4.6	3	170	120	Yes	7, monomeric	2–7
Luna™ C_8 (2)[c]	100×4.6	3	400	100	Yes	13.5, monomeric	1.5–10
Supelcosil™ LC318 C_{18}[d]	250×4.6	5	75	300	Yes	6, proprietary	2–7
Supelcosil™ LCPAH C_{18}[d]	100×4.6	3	170	120	Proprietary	proprietary	2–7.5
ODS-AL C_{18}[e]	150×4.6	5	335	120	No	17, monomeric	2–6
Vydac® 201TP™ C_{18}[f]	250×3.2	5	73	300	No	8 to 9, polymeric	2–7
Zorbax® Bonus-RP C_{14}[b]	250×4.6	5	180	80	Yes	9.3, monomeric	1–9
The Carotenoid Column™ C_{30}[e]	250×4.6	5	175	Proprietary	No	20, polymeric	2–6

[a] All stationary phase particles are spherical silica, except Vydac® 201TP™ C_{18} which is irregular silica. Data provided by vendors.
[b] Aglient Technologies (formerly Hewlett-Packard), Waldbronn, Germany.
[c] Phenomenex®, Torrance, CA, USA.
[d] Supelco, Bellefonte, PA, USA.
[e] YMC, Wilmington, NC, USA.
[f] Separations Group, Hesperia, CA, USA.

were clarified using 0.45-μm, PTFE, HPLC syringe cartridge filters fitted with glass fiber prefilters (Scientific Resources Inc., Eatontown, NJ, USA).

3. Results and discussion

3.1. Criteria for conditions used for collecting input data

The conditions used for collecting input data on each column are detailed in Table 2. We selected values of T between 40 and 60°C because these above-ambient temperatures are easily attainable by most column thermostatting devices and because our previous work [9,23,24] had indicated that these values of T provided resolution (R_s) between a great number of pigments. We felt that differences in T not greater than 20°C would be more likely to ensure accurate predictions as Sander and Wise [30] had observed that separation selectivity (α) does not necessarily change in a linear fashion over a wide range of T (−20 to 100°C). Temperatures we used do not necessarily result in the best R_s between all pigments. In fact, others have seen [9,13,14,16] that lower T values often improved R_s between selected pigments.

We selected values for t_G of 15 and 45 min or 20 and 60 min (Table 2) depending on column retentiveness. Some pigments eluted after the gradient and an isocratic hold on solvent B was necessary in these cases.

We used the same mobile phase with all columns as this study did not extend to the effects of mobile phase on separations. Thus we used methanol as solvent B even when a solvent of stronger elutropic strength may have been more practical, except with the C_{30} column. Because it was extremely retentive, it was necessary to change to a stronger solvent (ethanol).

Historically, many pigment separation methods have used a gradient system where solvent A is based on that of Mantoura and Llewellyn [5]: (80:20) methanol:0.5 *M* aqueous ammonium acetate and 0.025 *M* TBAA, pH 7.1. Many pigment analysts have subsequently deleted TBAA from solvent A [3,4,7–14,16–20,31] as reviewed in Jeffrey et al. [1]. During initial data collection we observed abnormal chl *a* retention (as with excessive chl *a* allomerization) when highly concentrated algal extracts and chl *a* standards were injected while ammonium acetate was used in solvent A without TBAA. This abnormal retention was eliminated by adding butylated hydroxy toluene (BHT) to the mobile phase (as suggested by an anonymous reviewer) or as we did, by replacing ammonium acetate with TBAA. We have avoided the costs ordinarily associated with the purchase of TBAA ion-pairing reagent by formulating it ourselves from the acidification of tetrabutyl ammonium hydroxide with acetic acid. TBAA was also advantageous in positioning the early eluting chlorophylls in front of the early eluting xanthophylls on the C_{30} column. In contrast, when ammonium acetate was used in solvent A, the early eluting chlorophylls were retained longer, eluted among the early eluting xanthophylls and caused many pigments to co-elute.

3.2. Column characteristics

Physical characteristics of the columns used were diverse (Table 3). Small particle sizes and long column dimensions generally increase column efficiency, N, while other stationary phase characteristics have a greater effect on α. Of the nine stationary phases used, two were listed by the vendors as polymeric and five as monomeric. The remaining two, the Supelcosil LC PAH and the LC 318, for which the bonding chemistry was listed as proprietary, were characterized as polymeric and monomeric, respectively, by Epler et al. [32].

Plate number (N) calculations for gradient data are complex but are conveniently calculated by the simulation software. Hence we easily compared N among columns. With DryLab one can enter the value of N observed during data collection or, as we did, enter various values of N until the accurate value is found (at which point the software predictions of peak width and R_s match those observed during data collection). Specifically, we used the peak widths and R_s of pairs eluting midway in the gradient from input data derived from the cooler T and longer t_G (Table 2) to identify the accurate value of N for each column. Next, we used the software to determine N for each column after normalizing the variables which affect N. Specifically, we entered the same

column dimension (250×4.6 mm), particle size (5 μm) and flow-rate (F=1 ml/min), as these varied among columns in the experimental procedures. In all cases, the monomeric columns were more efficient (with higher N values) than the polymeric C_{18} columns (Table 4). The columns with the highest efficiencies were the Luna C_8 and the Eclipse XDB C_8. We show no data for the C_{30} column as we had used a different mobile phase and thus the observed N (8500) cannot be compared exactly with values of N for the other columns.

We used the simulation software to compare the resolving power of each column free from the effects of their differences in N and column dimensions. Inspection of the R_s equation for gradient elution, $R_s = 1/4N^{1/2}(\alpha - 1)[k^*/(1 + k^*)]$ [33], reveals the interaction among N, α and k^*. In the computer simulation software, we normalized N and factors affecting k^* among columns. With these variables normalized, changes in R_s attained from manipulations to T or t_G reflect their effects on separation selectivity (α). The quantity k^* is defined by $(t_G F)/(V_m \Delta\phi S)$, where t_G is gradient time in min, $\Delta\phi$ the percent change in solvent B during the gradient divided by 100, F the flow-rate (ml/min), V_m the column volume (ml) and S is a constant that is a function of the molecular structure of each compound. We adjusted variables affecting k^* so that it was equal for each column by using a gradient range of 20–100% solvent B, F of 1 ml/min and column dimensions of 250×4.6 mm. Values of S can be assumed to be approximately equal for a given solute on different columns [34]. After normalizing k^*, we entered the same N value (10 000) for each column. Next we set t_G to 20 min (T=50°C) and used the simulation software to predict the R_s between adjacent pigments. The R_s predicted from the 20 min t_G was compared to the R_s predicted between the same pigment pairs when t_G was 60 min (T=50°C). We then used the simulation software to predict the R_s between adjacent pigments at 45°C (t_G=45 min) and calculated the change in R_s seen between the same pairs when T was set to 60°C (t_G=45 min.). We used the same pigments with each column and included only those that eluted during the gradient with all sets of conditions used. As a result, chlorophylls were excluded.

The effects of variations to t_G and T on the resolving power of each column are shown in Fig. 1. We illustrate the results with columns sorted first by bonding chemistry (either monomeric or polymeric) and second by aliphatic chain length (C_8 to C_{30}) (Fig. 1, x axis). (Note that data from the C_{30} column is not relevant to the other columns as previously stated.) The change in R_s associated with the 3-fold change in t_G (●) and the 15° difference in T (○) are shown (y axis). There was tremendous variability (as indicated by the distribution of data along the y axis) for both t_G and T for all columns. Changes in R_s resulting from T (○) were generally greater on the polymeric columns relative to the monomeric columns. In fact, the average median value of changes in R_s associated with T on the two C_{18} polymeric columns (1.17±0.12) was 3.7 times the average

Table 4
Observed values of N (derived from input data and experimental conditions given) and normalized values of N[a]

Column	Experimental conditions			N	
	Column dimensions (mm)	Particle size (μm)	Flow rate (ml/min)	Observed	Normalized
Eclipse XDB C_8	150×4.6	3.5	1.0	17 000	22 000
Luna C_8 (2)	100×4.6	3	0.8	10 500	21 850
Hypersil mos-2 C_8	100×4.6	3	1.0	8000	12 550
Bonus-RP C_{14}	250×4.6	5	1.2	10 500	10 250
LC318 C_{18}	250×4.6	5	1.0	15 000	15 000
ODS AL C_{18}	150×4.6	5	1.0	8800	14 800
201TP C_{18}	250×3.2	5	0.6	5250	4370
LC PAH C_{18}	100×4.6	3	1.0	2200	4400

[a] When normalizing N: column dimensions, 250×4.6 mm; particle size, 5 μm; and flow-rate, 1 ml/min.

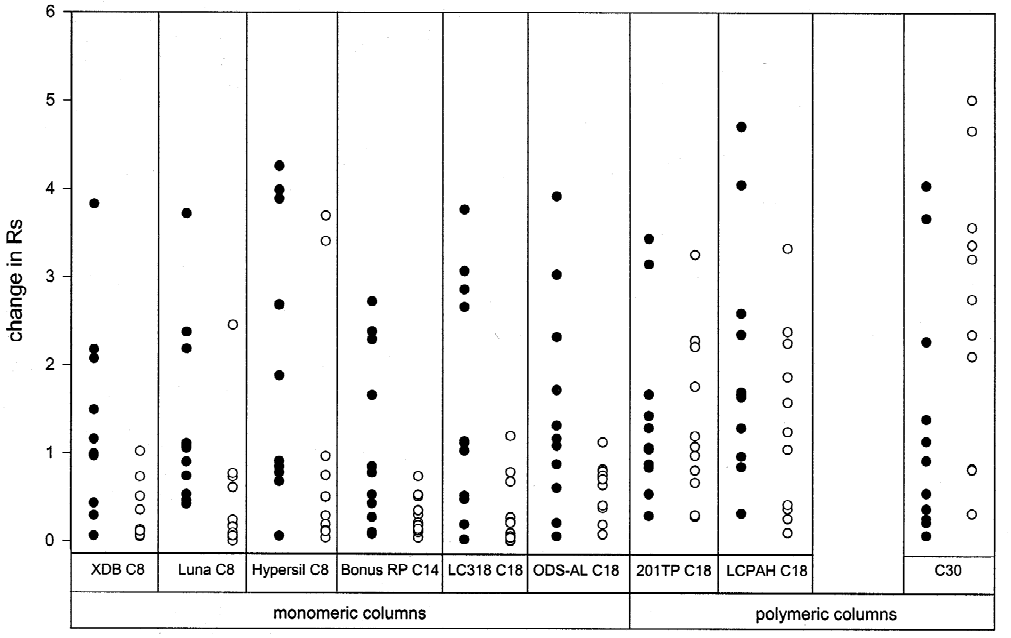

Fig. 1. Changes in R_s as a function of t_G or T. All data derived from computer simulations using the input data from each column. The theoretical change in R_s (y axis) resulting from two values of t_G (●), 20 and 60 min (where $T=50°C$) and the change in R_s resulting from two values of T (○), 45 and 60°C (where $t_G=45$ min) is shown for each column. Columns were normalized for factors that affect R_s (N and k^*; details in Section 3.2) prior to calculating R_s. Mobile phase: solvent A, 70:30 (v:v) methanol, 28 mM aqueous TBAA, pH 6.5; solvent B methanol for all but the C_{30} column (ethanol). Data from this column are therefore not directly comparable to the others.

median value associated with T on the monomeric columns (0.32 ± 0.23). Others have also demonstrated that phytoplankton pigment separations on polymeric columns are highly sensitive to changes in T [9,13–16]. The average median value of changes in R_s associated with t_G for the two C_{18} polymeric columns (1.37 ± 0.42) and the six monomeric columns (1.17 ± 0.38) were more similar relative to the differences seen with T. While data for the C_{30} column is not directly comparable to others, it was sensitive to both changes of T and t_G with somewhat greater sensitivity to T.

These data (Fig. 1) explore separation characteristics among columns independent of differences in N. However, factors affecting separations are only useful if peak widths are sufficiently narrow so that adequate R_s (ideally $\lesssim 1.5$) is attained. Highly efficient columns are therefore advantageous. In fact, the relatively large changes in R_s shown for the LC PAH C_{18} column (Fig. 1, where N was normalized to 10 000) were in reality unattainable as peak widths were abnormally broad during experimental conditions (observed $N=2200$). The low efficiency seen with this column may have resulted from an incompatibility with the conditions used. We show no subsequent data for this column.

While the independent effects of T and t_G are of interest, their combined effects are more important. The resolution map of the DryLab simulation software is most useful with its visual display of the R_s attainable at all possible combinations of t_G and T, as Dolan et al. [24] illustrated with 14 different samples (including algal pigments).

3.3. Using computer simulations to develop methods for pigment isolation

Our strategy for isolating pigment standards was to isolate as many as possible from the same source using methods which were fast and resulted in a final product of high chromatographic and peak purity. Here we demonstrate how we used computer simulations to develop methods for isolating pigments from

extracts of *G. galatheanum* and *T. pseudonana* combined.

For a column to be selected for pigment isolation, we required that it: (1) exhibit high sample capacity, (2) low back pressure, (3) high efficiency, (4) not excessively retain the latest eluting pigment in the extract (β,β-car) and (5) provide exaggerated R_s (>3.0) between pigments to be isolated. The LC 318 C_{18} stationary phase met our requirements and computer simulations indicated that the desired R_s could be achieved between a number of the 10 pigments to be isolated from this algal mixture. The simulation software also indicated that a shorter column (100 mm) would fulfil our requirements and shorten run times.

In Fig. 2A, we show the chromatogram produced on the LC 318 C_{18} column (100×4.6 mm) from the injection of the combined extract of *G. galatheanum* and *T. pseudonana*. The chl *c*3 (1), hex-fuco (15), diato (23), and the gyroxanthin diester-like (28 and 29) pigment fractions were collected free of contamination from this injection. Three impure fractions, chl *c*1, chl *c*2 and chlide *a* (5, 3, 6), but-fuco and fuco (9, 10) and diadino plus an unknown degradant (19+?) were collected and subsequently purified using other methods.

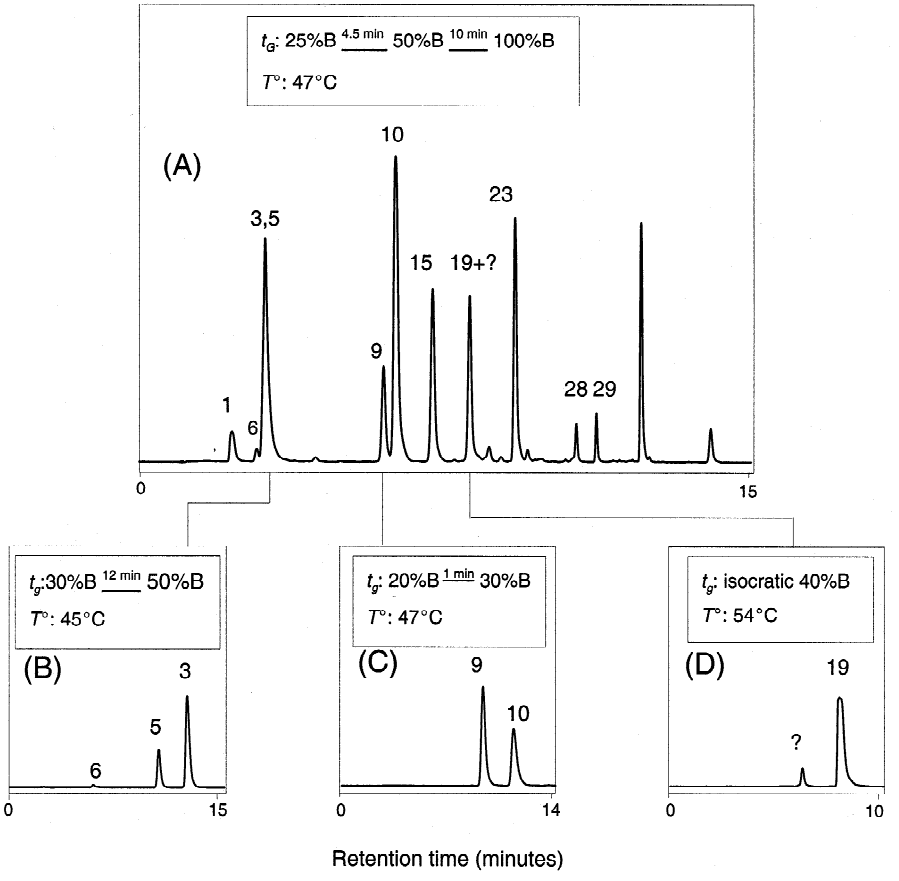

Fig. 2. Chromatograms from methods developed with the simulation software for the isolation of pigment standards from *T. pseudonana* and *G. galatheanum*. Peaks 1, 15, 23, 28 and 29 (identities in Table 1) were collected as pure fractions from the initial injection (A). Impure fractions were collected and subsequently purified on other methods (B–D). Mobile phase: solvent A, 70:30 (v:v) methanol, 28 m*M* aqueous TBAA, pH 6.5; solvent B, methanol. For the segmented gradient in (A) 50%B is reached at 4.5 min and 100%B at 10 min. Flow was individually adjusted to shorten run time. Columns used (details in Table 3): (A) LC 318 C_{18}, 100×4.6 mm; (B) C_{30}; (C,D) 201TP C_{18}. Inject volume 900 μl (sample premixed with buffer before injection).

For final purification of the three impure fractions, we developed methods using polymeric columns capable of achieving exaggerated R_s in short analysis times (Fig. 2B–D). The chl *c*1 (5) and chl *c*2 (3) fractions were each collected free of contamination from chlide *a* (6) with a method using the C_{30} column (Fig. 2B). We used the 201TP C_{18} column for isolating but-fuco (9) from fuco (10) (Fig. 2C) and diadino (19) free of contamination by the unknown pigment (Fig. 2D). After isolation, we transferred the pigments from the mobile phase in which they had been collected to the solvent required for use with the corresponding extinction coefficient. Chl *c*1 and *c*2 were transferred to acetone using solid-phase extraction [35]. The other pigments were transferred to ethanol by individually injecting each onto the C_{30} column with ethanol as the isocratic mobile phase and then collecting the pigment as it eluted from the column. We varied values of *T* to optimize the retention of each pigment such that the peak to be isolated was sufficiently removed from the injection peak and the run time was not excessively long.

Finally, the isolated standards were checked for chromatographic purity on each of two analytical methods using different columns (methods not shown). Chromatographic purity was >95% in all cases. Peak purity was also demonstrated by comparing the absorbance spectra on the peak upslope, apex and downslope attained from the HPLC in-line photo-diode array detector.

3.4. Optimizing pigment separations through changes to column temperature and gradient time

We used computer simulations to identify chromatographic conditions capable of resolving the greatest number of very important pigments in our test mixture. Some pigments in this mixture provide more meaningful information than others with regard to algal class diversity and abundance so we ranked them by their degree of importance as we anticipated that not all could be resolved in one analysis. Fourteen pigments classified as very important to resolve (those marked with **, Table 1) and 13 pigments considered less important to resolve (those marked with *, Table 1) were included in the test mixture. Pigments with no such notation (Table 1) and in our test mixture (peak codes 8, 32–34, 40 and 41, Table 1) were considered as interference peaks only. We sought fast methods, rejected analysis times greater than 60 min as impractical even if the longer analysis times improved separations and avoided segmented gradients in favor of simple linear gradients. We emphasize that the values of *T* and t_G available for use were constrained by the conditions used while collecting input data and are not necessarily optimal for all pigment pairs.

Analyses were conducted on each of eight columns using the chromatographic conditions identified in DryLab. The resulting chromatograms and conditions used are illustrated (Figs. 3–6). No column was able to resolve all pigments ($R_s \geq 1.0$) in the same analysis. The co-eluting pigments seen with each method are summarized (Table 5).

Only the C_{30} column was capable of separating all pigments (with ** or *, Table 1) in our test mixture, albeit not in one run (Fig. 3A,B). With simple manipulations to t_G and *T*, this column resolved all chlorophylls (Fig. 3A) and all carotenoids and xanthophylls (Fig. 3B). We used a segmented gradient in Fig. 3B simply to shorten run time. The other polymeric column, the 201TP C_{18}, achieved separation between the maximum number of carotenoids at 60°C. Others have shown that at subambient [9,14,16] and ambient [13] temperatures, this column can resolve the chlorophyll pigments not resolved here.

The co-elution of some pigment pairs was related to the aliphatic chain length of the stationary phase. For example, the separation of monovinyl chl species (chl *c*1 and chl *a*) from their divinyl counterparts (chl *c*2 and DV chl *a*) was achieved easily on the C_{30} and C_8 columns but not on others (DV chl *b* and chl *b* were resolved only on the C_{30} column). β,ε-car and β,β-car were resolved on all but the C_8 columns. The co-elution of these carotene pigments is of little importance in describing algal class diversity in natural samples; however, the identification of DV chl *a* in a natural sample uniquely indicates the presence of prochlorophytes and therefore this separation is very important in the analysis of oceanic samples.

The co-elution of other pigments did not seem to correlate with stationary phase aliphatic chain length. The Hypersil C_8 and the LC 318 C_{18} (Fig. 4A,B) did

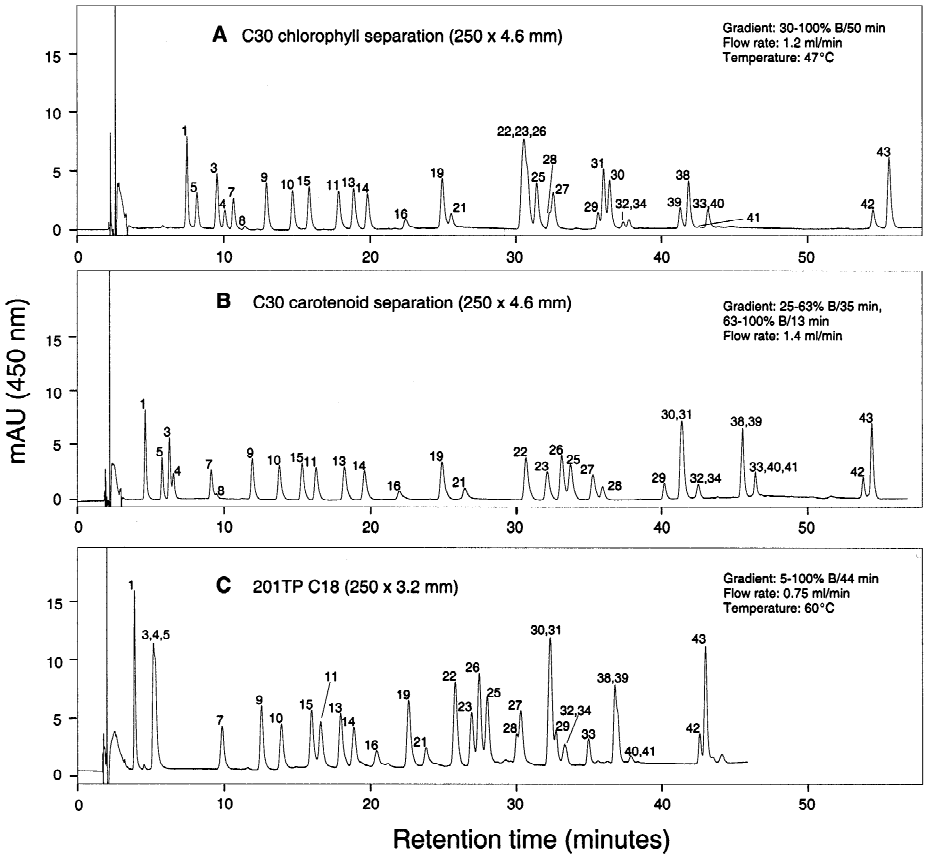

Fig. 3. Separations of pigments in a test mixture from methods developed with the simulation software for use with two polymeric columns. Separations were developed for the C_{30} column to separate all chlorophylls (Fig. 3A) and to separate all carotenoids and xanthophylls (Fig. 3B). The separation shown in Fig. 3C was developed for the 201TP C_{18} column to separate the maximum number of very important pigments in the shortest analysis time. Experimental conditions: mobile phase-solvent A, 70:30 (v:v) methanol, 28 m*M* aqueous TBAA, pH 6.5; solvent B, methanol (except (A,B) when it was ethanol); column details in Table 3; peak identities in Table 1.

not resolve neo, pras, and viola (11, 13, 14). Resolution between lut and zea (26, 25) was the most limiting ($R_s = 0.6$) with the Bonus-RP C_{14} and the ODS-AL C_{18} (Fig. 5A,B); somewhat limiting (R_s $1.0 \geq 1.2$) on the other C_{18} columns (Figs. 3C and 4B) and the C_{30} column (Fig. 3B); and the best ($R_s \geq 1.5$) with the C_8 columns (Figs. 4A, 6A and 6B). Resolution between lut and zea was easily improved on the two polymeric columns (the C_{30} and the 201TP C_{18}) with changes to *T* at the expense of decreases in R_s between other pigments. With the ODS-AL C_{18}, trends seen on the resolution map (not shown) for this column hinted that temperatures <40°C (not available for use with simulations) may have been advantageous for resolving lut from zea. Thus, it is unfortunate that we had not evaluated this column at near-ambient temperatures. The Luna C_8 and the Eclipse XDB C_8 columns provided separations of the maximum number of very important pigments in one analysis (Fig. 6A,B and Table 5).

3.5. Accuracy of computer simulations

We found, as have others [33,36], the computer simulations to be highly accurate when comparing observed data with predicted data. Ghrist et al. [37] found that prediction accuracy was best when input data and modeled data were collected close together in time. We observed an average deviation between predicted and observed t_R values of 0.06 and 0.18

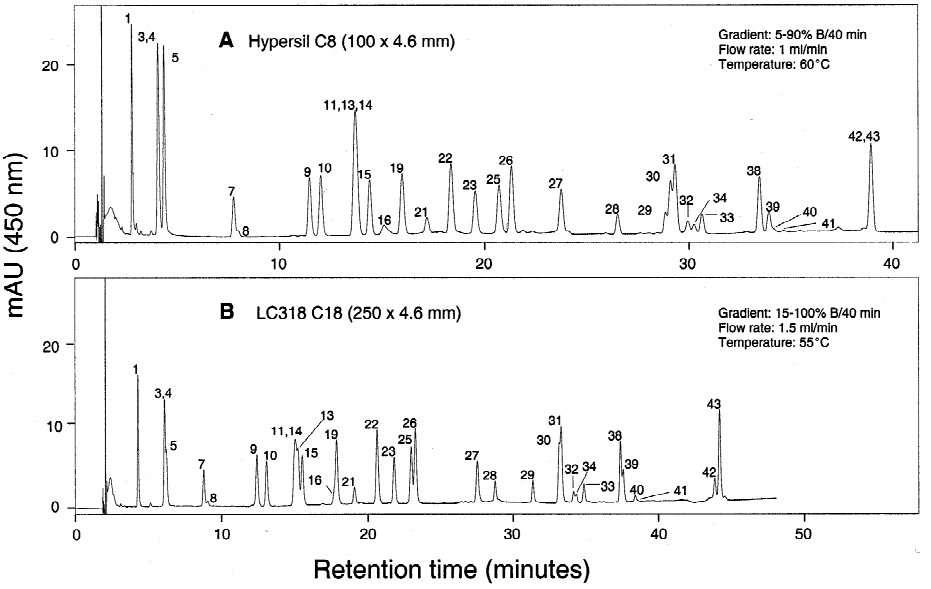

Fig. 4. Separation of pigments in the test mixture on two columns that were unable to resolve neo, pras and viola. Methods were developed for the (A) Hypersil C_8 and (B) LC 318 C_{18} columns for the purpose of separating the maximum number of very important pigments in the shortest analysis time (experimental details in Fig. 3 legend).

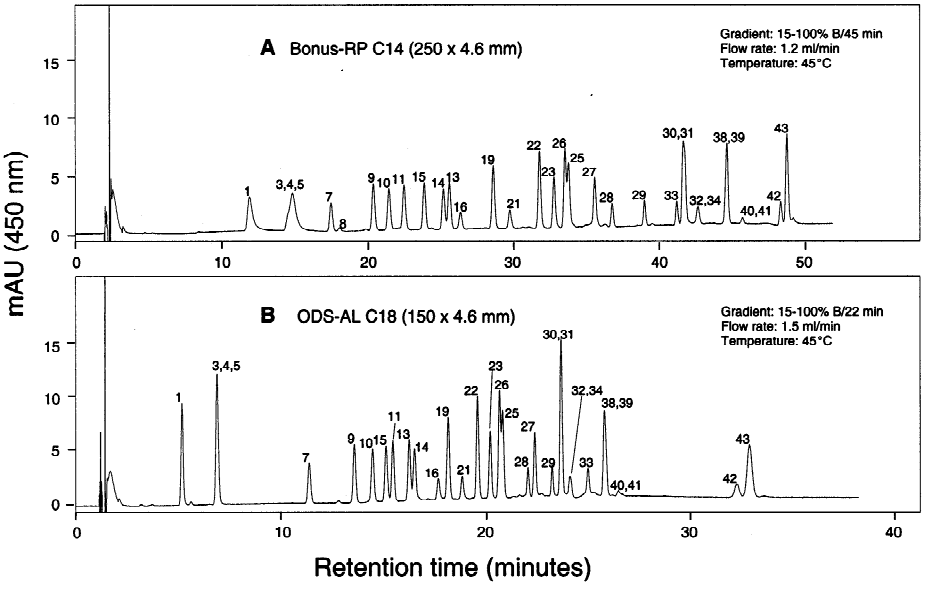

Fig. 5. Separation of pigments in the test mixture on two columns that had difficulty resolving lut and zea. Methods were developed for the (A) Bonus-RP C_{14} and (B) ODS-AL C_{18} columns for the purpose of separating the maximum number of very important pigments in the shortest analysis time (experimental details in Fig. 3 legend).

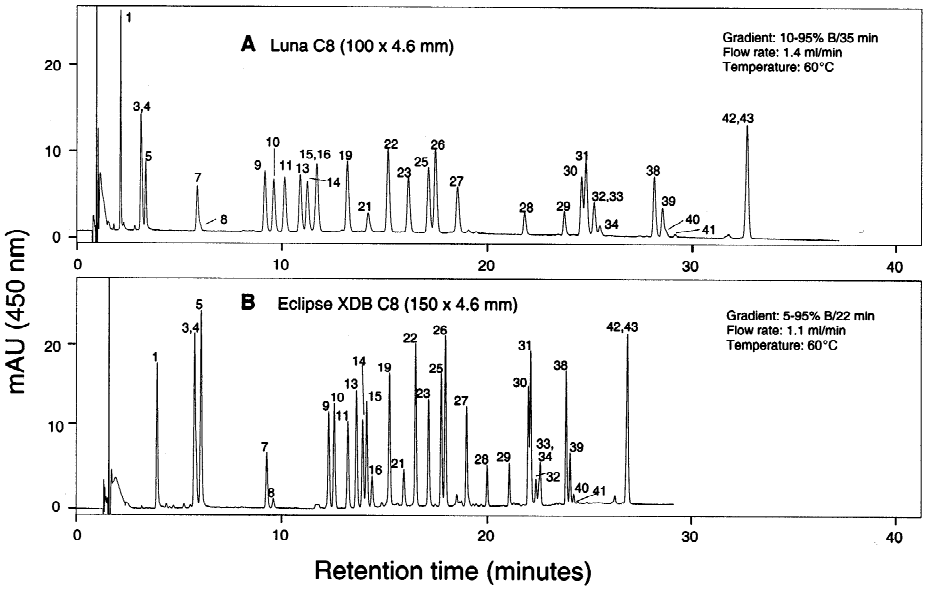

Fig. 6. Separation of pigments in the test mixture on two columns that, relative to the columns in Fig. 3, 4 and 5 separated the most pigments in one run. Methods were developed for the (A) Luna C_8 and (B) the Eclipse XDB C_8 columns for the purpose of separating the maximum number of very important pigments in the shortest analysis time (experimental details in Fig. 3 legend).

min (using all pigments but chl *c*3) when input data and experimental data were collected either within 2 days or up to 21 days, respectively. When all early eluting chlorophylls were excluded from the average, the deviation dropped by 50% in both cases. Injector programming and large injection volumes (especially

Table 5
Pigments in the column test mixture that co-eluted, as shown in Figs. 3–6 (columns and conditions therein described)[a]

Co-eluting pigments (pigment codes)	Columns featured in Figs. 3 through 6								
	Fig. 3A C_{30}	Fig. 3B C_{30}	Fig. 3C 201TP C_{18}	Fig. 4A Hypersil C_8	Fig. 4B LC318 C_{18}	Fig. 5A Bonus-RP C_{14}	Fig. 5B ODS-AL C_{18}	Fig. 6A Luna C_8	Fig. 6B XDB C_8
Chl *c*2, Mg DVP, chl *c*1 (3, 4, 5)			x		x	x	x		
Chl *c*2, Mg DVP (3, 4)			x	x	x	x	x	x	x
Neo, pras, viola (11, 13, 14)				x	x				
Hex-fuco, asta (15, 16)								x	
Asta, diadino (16, 19)					x				
Allo, diato, lut (22, 23, 26)	x								
Zea, Lut (25, 26)						x	x		
Cantha, gyroxanthin-like (27, 28)	x		x						
Gyroxanthin-like, chl *b* (29, 31)	x								
Gyroxanthin-like, DV chl *b*, chl *b* (29, 30, 31)			x	x					
Chl *b*, DV chl *b* (30, 31)		x	x	x	x	x	x	x	x
DV chl *a*, chl *a* (38, 39)		x	x		x	x	x		
β,ε-car, β,β-car (42, 43)				x				x	x
No. of very important pigments resolved	10	11	10	10	8	9	9	12	13

[a] Co-elution of interference peaks (8, 32–34, 40 and 41) are not indicated here as they were resolved from important pigments (except for occasional co-elution of DV chl *a*′ with chl *a*). Pigments are considered unresolved when $R_s < 1.0$. Pigment codes and their relative importance are shown in Table 1.

when injection solvent is different from the initial mobile phase) create a micro-environment at the head of the column, which has the potential to alter t_R values and peak widths of early eluting compounds, independent of effects resulting from the mobile phase gradient and *T*. In fact, the simulation software often flagged early eluting chlorophylls as exhibiting abnormal chromatographic behavior.

3.6. A new method for the analysis of phytoplankton pigments in natural samples

We selected the method developed for the Eclipse XDB C_8 column for further testing for suitability in the routine quantitative analysis of phytoplankton pigments in natural samples. We chose this method because it provided the fastest analysis time, highest efficiency, maximum number of pigments resolved in one analysis and low solvent use relative to other methods tested. We identified the elution position of additional pigments, evaluated features important to quantitative analysis and demonstrated transferability.

As one is never certain what pigments may be present in natural samples, we analyzed extracts of additional algal monocultures (Fig. 7) containing pigments not in our test mixture to increase the library of pigments whose t_R values were documented by this method. We note several pigments that we could not identify (peak 18 and those listed with letters above the peaks, Fig. 7 and Table 1) but had the potential for co-elution with important pigments. For example, a pigment (18) with myxo-like spectra (Fig. 7E) co-eluted with diadino. Furthermore, extracts of *C. polylepsis*, *E. huxleyi* and *I. galbana* were analyzed on the XDB C_8 column and then again on the C_{30} column to examine the elution position of certain pigments. Data from the C_{30} column (not shown) enabled us to see that in *I. galbana* there were two additional pigments unknown to us (k and L in Fig. 7L and Table 1) imbedded in phytyl-chl *c* (37). Also, in *C. polylepsis* there were two pigments of identical spectra (m in Fig. 7I and Table 1) eluting as a shoulder on the front of chl *a* (39). Phytyl-chl *c* (37) from *E. huxleyi* (Fig. 7K) and *I. galbana* (Fig. 7L) each contained two identical fractions when analyzed on the C_{30} column.

Some additional pigments which we could identify co-eluted with others already identified. These include 4k-hex-fuco (12) shown in Fig. 7K (separated in [20]) that co-eluted with neo; phytyl-chl *c* (37) shown in Fig. 7K,L that co-eluted with chl *a* allom 2 (36) shown in Fig. 9A; and chlide *a* (6) shown in Fig. 7A, F and H that co-eluted with chl *c*1. As the quantitation of chlide *a* is important when reporting equivalent total chl *a* values, we suggest quantitation of chlide *a* (in the presence of chl *c*1) by using a dichromatic equation as in Latasa et al. [38] based on simultaneous monitoring of two different wavelengths (665 and 450 nm). (Note: we have subsequently determined that chlide *a* and chl *c*1 can be separated by increasing the molarity of TBAA.)

We evaluated factors important to quantitative analysis including such things as peak area and t_R reproducibility and minimum detection limits (MDL) [29]. We used data from seven replicate injections of a mixed standard containing 17 pigments ranging in concentration from 1.5 to 5.6 ng/injection (S/N varied from 20 to 70) for this evaluation. Peak area and t_R reproducibility averaged 0.75 %RSD and 0.04 %RSD, respectively. The average MDL of all 17 pigments evaluated was 0.06 ± 0.03 ng per injection. Additionally we tested 14 chl *a* calibration curves on six different XDB C_8 columns and found the mean slope to be 3.436 ± 0.046 (1.325 %RSD). Linear dynamic range was observed from 0.5 to >700 ng of pigment per injection (where 0.5 ng chl $a = S/N$ of 10 at 665 ± 10 nm). We demonstrate the suitability of this method for the analysis of dilute oceanic samples where total chl *a* abundance (DV chl *a* plus chl *a*) was 0.08 μg/l of seawater (Fig. 8).

We successfully transferred this method to a different HPLC (Beckman Gold) and laboratory (data courtesy of Ivy Collins and Alan Lewitus, University of South Carolina, Charleston, SC). We also tested the transfer to an HPLC with a high dwell volume by imposing an isocratic hold on initial conditions on our existing HPLC such that it mimicked an HPLC with a 10 ml dwell volume. This simulation also yielded results which were comparable to the original HPLC (Fig. 9).

Initial attempts to transfer this method to the Beckman Gold HPLC were unsatisfactory, as R_s between several peaks was poor. The column heater used with the Beckman Gold HPLC was a stand-

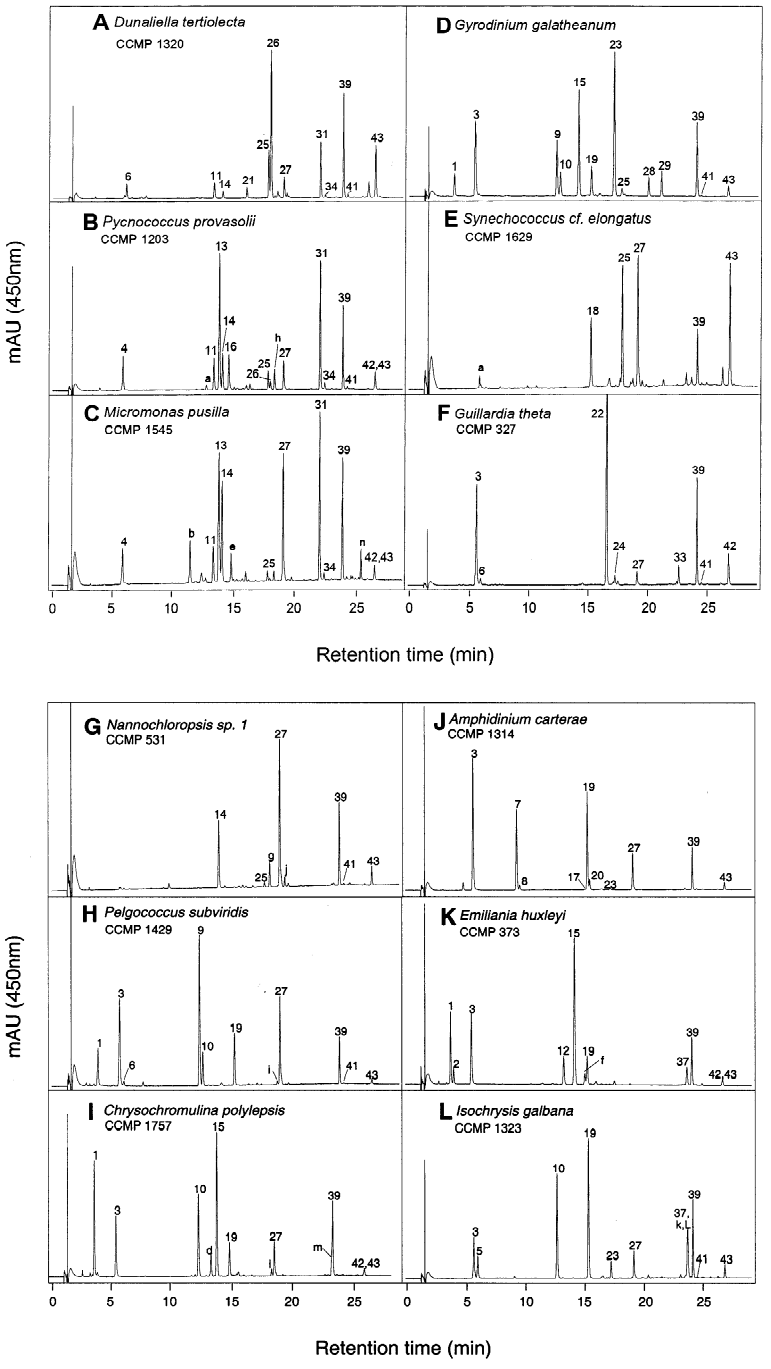

Fig. 7. Chromatograms of algal monocultures from various algal classes analyzed on the Eclipse XDB C_8 column showing the elution position of additional pigments not previously shown with the same method (Fig. 6B). Column details in Table 3; peak identities in Table 1. All cultures except *Gyrodinium galatheanum* (D), which was grown at Horn Point Laboratory, were from the Provasoli-Guillard Culture Collection (CCMP). Canthaxanthin (27) was added as an internal standard to all cultures except those depicted in Fig. 7D and K. Data courtesy of Ajit Subramaniam (Department of Meteorology, UMD, College Park, MD, USA) and Robert Vaillancourt and Robert Guillard (Bigelow Laboratory for Ocean Science, West Boothbay Harbor, ME, USA).

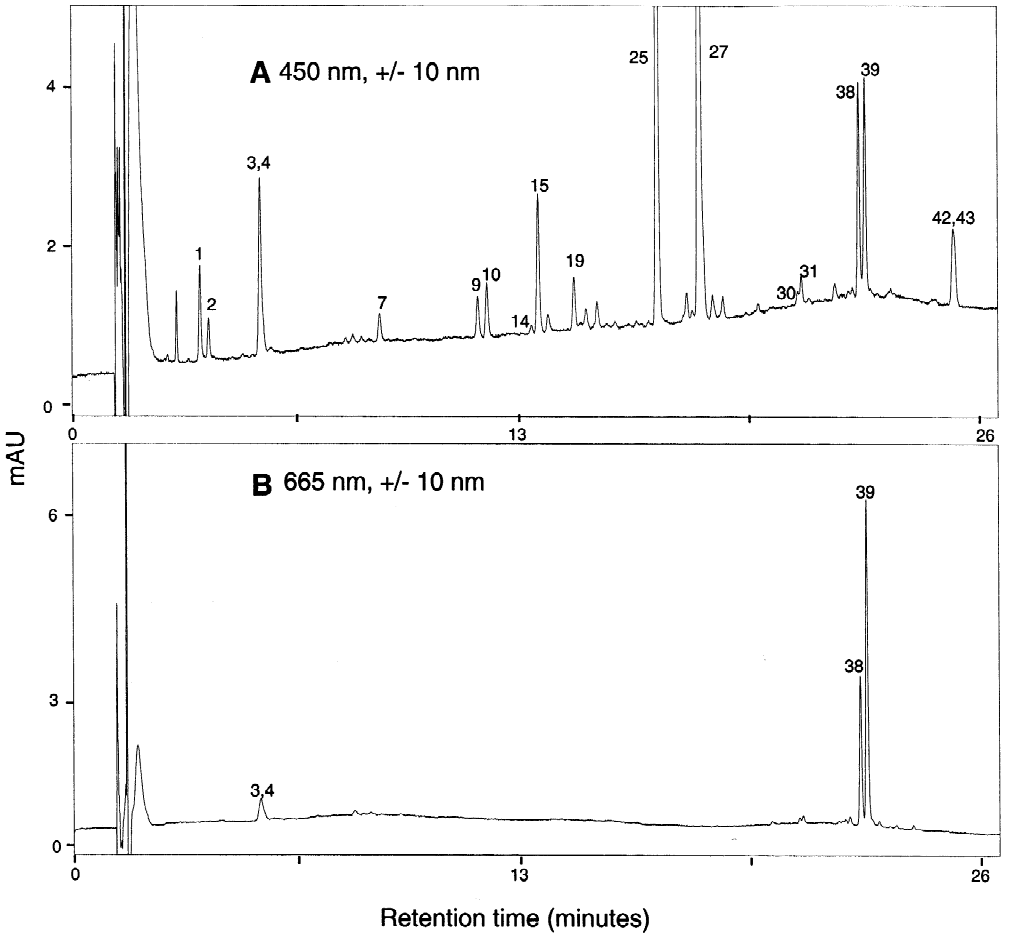

Fig. 8. Dilute natural sample analyzed on the Eclipse XDB C_8 column. DV chl *a* (38) is approximately 2 ng per injection and chl *a* (39) 6 ng per injection Column details in Table 3; pigment identities in Table 1. The sample was collected at 37°29.41′N, 73°23.00′W, which is 250 km ENE of the mouth of Chesapeake Bay (data courtesy of Lawrence Harding, Jr., Horn Point Laboratory, UMCES, Cambridge, MD, USA). Analyses using this method are also shown in Figs. 6B and 7.

alone unit which suspended the column in air inside. The solvent inlet line was not preheated and *T* was monitored by a glass mercury thermometer inserted into the column heater box.

Wolcott et al. [39] noted several reasons for the ineffective transfer of methods between instruments when elevated column temperatures (>40°C) are used. Of these reasons, the most likely to have adversely affected our ability to initially transfer this method to the Beckman HPLC were column thermostat inaccuracy and lack of mobile phase preheating prior to the column inlet (the latter of which causes temperature gradients within the column and a column *T* lower than expected). Column performance equivalent to that seen with our HP HPLC was achieved by increasing the column heater set-point from 60 to 61.5°C and by inserting a piece of stainless steel tubing (100 cm long×0.007′ I.D.) between the injector and the column with approximately 82 cm coiled within the column heating box so that the mobile phase was pre-heated to the column *T*.

4. Conclusions

The present study shows that method development software (DryLab) can be used to identify methods

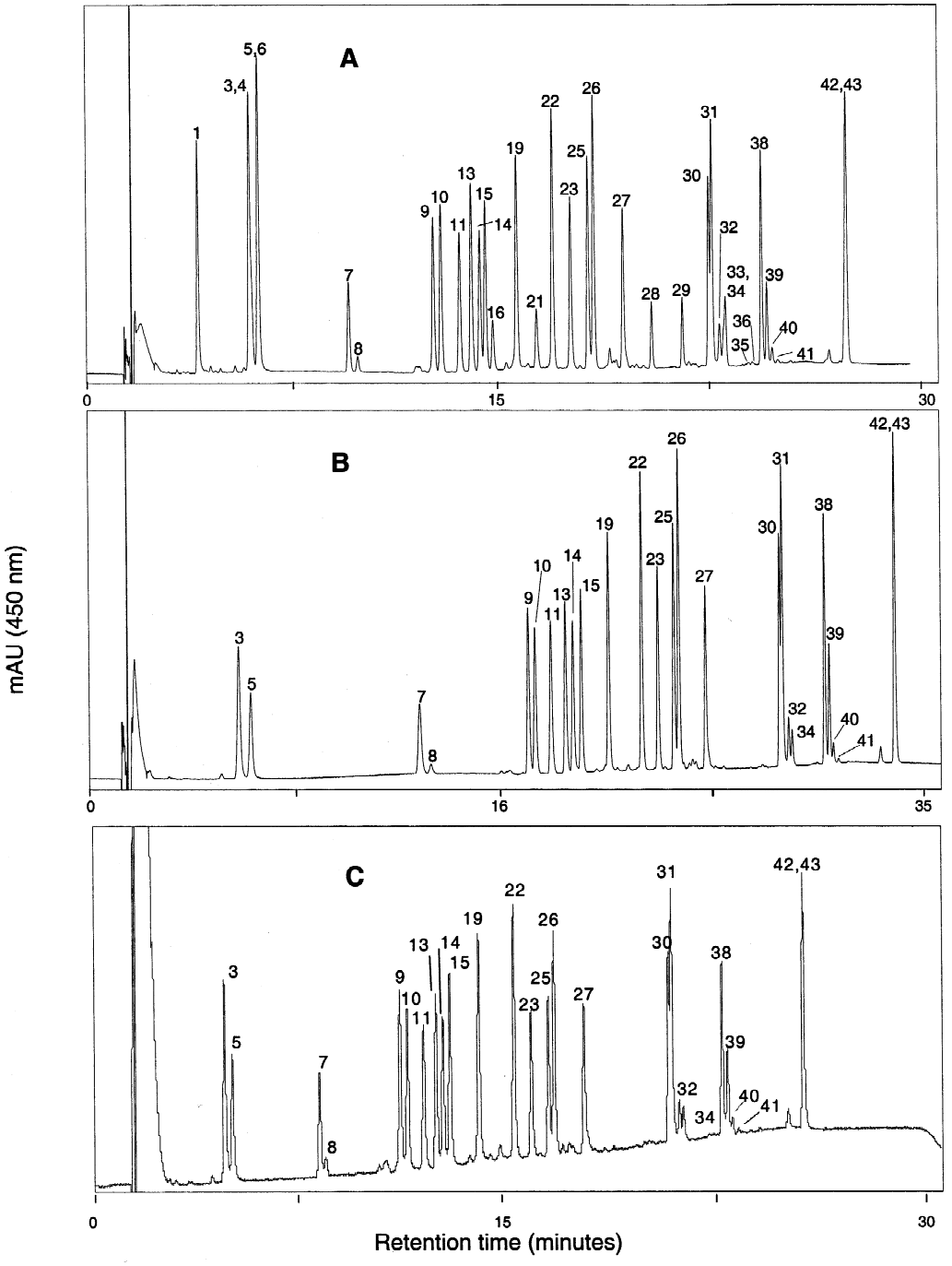

Fig. 9. Chromatograms showing transferability of the method developed for the Eclipse XDB C_8 column. Column details in Table 3; peak identities in Table 1. Some pigments were present in (A) but not in (B,C). (A) HP 1100 HPLC, dwell vol = 3 ml; (B) HP 1100 HPLC, dwell vol = 10 ml (simulated); (C) Beckman Gold HPLC, dwell vol = 2.2 ml. Mobile phase: solvent A, 70:30 (v:v) methanol, 28 m*M* aqueous TBAA, pH 6.5; solvent B, methanol. $F = 1.1$ ml/min. T (A,B) = 60°C; T (C) = 61.5°C. Gradient conditions in (A,C): linear gradient of 5–95% B in 22 min followed by an isocratic hold for 7 min and return to initial conditions in 2 min; in (B), initial conditions (5% solvent B) were held isocratically for 6.4 min to simulate a 10 ml dwell volume before starting the gradient. Methods in (A,B) used an injector program; in (C) the sample was premixed with buffer (50:50) and manually injected (200 μl).

useful for the isolation and analysis of phytoplankton pigments on columns varying greatly in stationary phase physical characteristics and that changes to column T and t_G alone effectively enhance separations. It is unlikely, however, that the separations we identified are the best attainable for each column as we did not explore the use of other mobile phases and, as we limited our choice of T to what is conveniently attained with most column heating devices, we did not evaluate the effects of ambient or sub-ambient T on these columns.

Changes in R_s seen with adjustments to T were profound on the polymeric columns (relative to the monomeric columns) where changes of T as little as 5°C caused otherwise well-resolved peaks to co-elute. The modeling software was especially useful with the polymeric columns, as many pigments pairs were greatly affected by changes in T and optimal conditions were confined to a fairly narrow range of T and t_G in many cases. This sensitivity to T is advantageous when collecting pigments to be isolated as standards (where exaggerated R_s is required between selected pigments), or when attempting to gain information about peaks that are unresolved on the primary method used (as we did with pigments found in the extracts of *I. galbana*, *E. huxleyi* and *C. polylepsis* analyzed first on our primary method with the XDB C_8 column and secondly on the C_{30} column). Extreme sensitivity to T can be disadvantageous, however, when attempting to reproduce methods between instruments, as inaccuracies in column thermostatting devices can result in unexpected changes to α. Strict adherence to the guidelines set forth by Wolcott et al. [39] is mandatory for success in transferring methods when using elevated column T. We do not advise using polymeric columns without controlling T.

We found that a two-step procedure for the isolation of pigments for use as standards from a complex matrix was very time efficient and produced products of high quality. A highly efficient monomeric column with low back-pressure and high sample capacity (such as the Supelcosil LC 318 C_{18} column) was useful for the isolation of crudely purified fractions when pigments of interest co-eluted, or for the isolation of well-resolved pigments. Partially purified fractions were subsequently re-injected and the constituent pigments isolated as pure fractions from columns (primarily polymeric ones) with selectivities that differed from the LC 318 C_{18} column. We isolated 20 different pigments using methods based on these principles.

From our survey of columns (Figs. 3–6), we found the XDB C_8 column combined high efficiency (important to good detectability) and desirable α. We regret that the additional pigments identified from the analysis of culture extracts (Fig. 7) were not included in the input data from which our T and t_G conditions were derived, as we were unable to determine if other conditions would have been more optimal for resolving the pigment pairs observed to co-elute (Table 1) with conditions used. The method described for this column is well suited to the analysis of pigments in dilute or highly concentrated natural samples as the method has excellent detectability and the linear dynamic range extends to the point of detector saturation. The analysis time is convenient (27 min for elution of the most retained pigment). The method uses a simple mobile phase (composed primarily of an inexpensive organic solvent, methanol) and a linear gradient (which contributes to baseline stability). Because the peak shape, and therefore R_s, of early eluting chlorophylls is affected by injection conditions and injector capabilities, analysts may need to individualize injector programs, ratios of solvent to buffer and injection volumes to achieve similar results for these pigments. This method has been used extensively in our laboratory for the analysis of natural samples and has exhibited excellent column to column reproducibility with regard to α, R_s and response factor stability. This method was recently evaluated in an intercalibration exercise [40] and compared favorably with other methods tested.

Acknowledgements

We gratefully acknowledge Victor S. Kennedy for encouragement and editing of our manuscript and Hugh MacIntyre for his comments as well; Garry Baptist, Dan Gustafson, Stacy Kane, Aishou Li, Deborah Kennedy and William Severn for algal cultures grown at Horn Point and Robert Vaillancourt and Robert Guillard for sharing data from their algal cultures grown at Provasoli-Guillard Center for

Culture of Marine Phytoplankton (CCMP); Lawrence Harding, Jr. and Ajit Subramaniam for shared data; Ivy Collins and Alan Lewitus for testing the transferability of our method, through EPA grant # R826944-01-0; Agilent Technologies, Phenomenex, The Separations Group, Supelco and YMC for donations of columns; LC Resources, Inc. for their donation of DryLab; Perdue, Inc. for donations of the pigments lutein and canthaxanthin; Lloyd Snyder of LC Resources for his help with improving column heater performance and solving chromatographic problems and for his suggestions and guidance with data analysis and interpretation (Section 3.2); Simon Wright for his assistance with tentative identification of pigments (unknown to us) in *Emiliana huxleyi*; Patricia Glibert (Analytical Services Chairperson) and Thomas Malone (Laboratory Director) for their continuing support of our efforts to improve methods; and the anonymous reviewers. This work was partially funded by ONR award No. N000140010151. This is contribution No. 3381 from the University of Maryland Center for Environmental Science.

References

[1] S.W. Jeffrey, S.W. Wright, M. Zapata, Mar. Freshwat. Res. 50 (1999) 879.
[2] M. Olaizola, J. La-Roche, Z. Kolber, P.G. Falkowski, Photosyn. Res. 41 (1994) 357.
[3] G.W. Kraay, M. Zapata, M.J.W. Veldhuis, J. Phycol. 28 (1992) 708.
[4] S.W. Wright, S.W. Jeffrey, R.F.C. Mantoura, C.A. Llewellyn, T. Bjornland, D. Repeta, N. Welschmeyer, Mar. Ecol. Prog. Ser. 77 (1991) 183.
[5] R.F.C. Mantoura, C.A. Llewellyn, Anal. Chim. Acta 151 (1983) 297.
[6] S.W. Wright, J.D. Shearer, J. Chromatogr. 294 (1984) 281.
[7] M. Zapata, A.M. Ayala, J.M. Franco, J.L. Garrido, Chromatographia 23 (1987) 26.
[8] L. Van Heukelem, A.J. Lewitus, T.M. Kana, N.E. Craft, J. Phycol. 28 (1992) 867.
[9] L. Van Heukelem, A.J. Lewitus, T.M. Kana, N.E. Craft, Mar. Ecol. Prog. Ser. 114 (1994) 303.
[10] J.L. Garrido, M. Zapata, Chromatographia 35 (1993) 543.
[11] J.L. Garrido, M. Zapata, J. High Res. Chromatogr. 16 (1993) 229.
[12] S.L. Strom, Deep-Sea Res. 40 (1993) 57.
[13] J.L. Garrido, M. Zapata, S. Muniz, J. Phycol. 31 (1995) 761.
[14] K. Van Lenning, J.L. Garrido, J. Aristegui, M. Zapata, Chromatographia 41 (1995) 539.
[15] J.L. Garrido, M. Zapata, J. Chromatogr. 738 (1996) 285.
[16] J.L. Garrido, M. Zapata, Chromatographia 44 (1997) 43.
[17] R. Goericke, D.J. Repeta, Mar. Ecol. Prog. Ser. 101 (1993) 307.
[18] F. Vidussi, H. Claustre, J. Bustillos-Guzman, C. Cailiau, J.C. Marty, J. Plankton Res. 18 (1996) 2377.
[19] R.G. Barlow, D.G. Cummings, S.W. Gibb, Mar. Ecol. Prog. Ser. 161 (1997) 303.
[20] M. Zapata, F. Rodriguez, J.L. Garrido, Mar. Ecol. Prog. Ser. 195 (2000) 29.
[21] L.C. Sander, K.E. Sharpless, M. Pursch, J. Chromatogr. A. 880 (2000) 189.
[22] H. Schmid, H.B. Stich, J. Appl. Phycol. 7 (1995) 487.
[23] P.L. Zhu, J.W. Dolan, L.R. Snyder, N.M. Djordevic, D.W. Hill, J.-T. Lin, L.C. Sander, L. Van Heukelem, J. Chromatogr. A 756 (1996) 63.
[24] J.W. Dolan, L.R. Snyder, N.M. Djordevic, D.W. Hill, D.L. Saunders, L. Van Heukelem, T.J. Waeghe, J. Chromatogr. A 803 (1998) 1.
[25] S.W. Jeffrey, R.F.C. Mantoura, S.W. Wright (Eds.), Phytoplankton Pigments in Oceanography: Guidelines to Modern Methods, UNESCO, Paris, 1997, p. 447, Part IV.
[26] S.W. Jeffrey, R.F.C. Mantoura, S.W. Wright (Eds.), Phytoplankton Pigments in Oceanography: Guidelines to Modern Methods, UNESCO, Paris, 1997, p. 563, Appendix A.
[27] A. Li, D.K. Stoecker, J. Adolf, Aquat. Microb. Ecol. 19 (1999) 163.
[28] M.B. Bazzaz, Photochem. Photobiophys. 2 (1981) 199.
[29] D.C. Hurd, D.W. Spencer (Eds.), Marine Particles: Analysis and Characterization, American Geophysical Union, Washington, DC, 1991, p. 119, Chapter 4.
[30] L.C. Sander, S.A. Wise, Anal. Chem. 61 (1989) 1749.
[31] F. Rodriguez, M. Zapata, J.L. Garrido, Chromatographia 48 (1998) 677.
[32] K.S. Epler, L.C. Sander, R.G. Ziegler, S.A. Wise, N.E. Craft, J. Chromatogr. 595 (1992) 89.
[33] L.R. Snyder, J.W. Dolan, Adv. Chromatogr. 38 (1998) 115.
[34] J.W. Dolan, L.R. Snyder, T. Blanc, L. Van Heukelem, J. Chromatogr. A 897 (2000) 37.
[35] S.W. Jeffrey, R.F.C. Mantoura, S.W. Wright (Eds.), Phytoplankton Pigments in Oceanography: Guidelines to Modern Methods, UNESCO, Paris, 1997, p. 207, Chapter 7.
[36] J.W. Dolan, L.R. Snyder, R.G. Wolcott, P. Haber, T. Baczek, R. Kaliszan, L.C. Sander, J. Chromatogr. A 857 (1999) 41.
[37] B.F.D. Ghrist, B.S. Cooperman, L.R. Snyder, J. Chromatogr. 459 (1988) 1.
[38] M. Latasa, R.R. Bidigare, M.E. Ondrusek, M.C. Kennicutt II, Mar. Chem. 51 (1996) 315.
[39] R.G. Wolcott, J.W. Dolan, L.R. Snyder, J. Chromatogr. A. 869 (2000) 211.
[40] S.B. Hooker, E.R. Firestone (Eds.), Vol. 14, Sessions, 2000: The first SeaWiFS analysis round-robin experiment (SeaHARRE-1), NASA Tech. Memo. 2000-206892, NASA, Greenbelt, MD, in press, SeaHARRE-1.